



THE IMPACT OF RISING ATMOSPHERIC CO<sub>2</sub> LEVELS AND RESULTING OCEAN ACIDIFICATION  
TO THE PHYSICAL (SOLUBILITY) OCEAN PUMP OF CO<sub>2</sub>.

1

Wolfgang Dreybrodt

2

Faculty of Physics and Electrical Engineering, University of Bremen, Germany

3

[dreybrodt@ifp.uni-bremen.de](mailto:dreybrodt@ifp.uni-bremen.de)

4

5

6

7 **Abstract**

8

An alternative measure of the ocean's carbonate buffer system efficiency to absorb CO<sub>2</sub>

9

from the atmosphere is proposed. Instead of the Revelle factor  $R = (\Delta\text{CO}_2/\text{CO}_2)/(\Delta\text{DIC}/\text{DIC}) =$

10

$(\text{DIC}/\text{CO}_2)/(\Delta\text{DIC}/\Delta\text{CO}_2)$  the sensitivity  $S = (\Delta\text{DIC}/\Delta\text{CO}_2)$  is preferable because it gives

11

directly the change  $\Delta\text{DIC}$  of the concentration of DIC in the seawater caused by the change

12

$\Delta\text{CO}_2$  of carbon dioxide in the atmosphere. To this end the DIC concentration of seawater at

13

temperature  $T$  in equilibrium with a defined CO<sub>2</sub> level in the surrounding atmosphere is

14

calculated by use of the geochemical program PHREEQC. From the function  $\text{DIC}(\text{CO}_2, T)$  one

15

obtains by differentiation the sensitivity  $S = d\text{DIC}/d\text{CO}_2 = \Delta\text{DIC}/\Delta\text{CO}_2$  and also the Revelle

16

factor  $R$ . Using  $S$  as the change of the ocean's buffer capacity reveals a better insight of its

17

future evolution than using the Revelle factor  $R$ .

18

One finds that the buffer capacity  $S$  has declined by about 30% from 1945 to present and

19

that its future decline from 400 to 600 ppm will be a further 30%. By calculating the uptake

20

of CO<sub>2</sub> of his equilibrium pump an upper value of 1.3 Gigatons/year is obtained, small in

21

comparison to the 10 Gigatons/year absorbed by the ocean at present. The Revelle factor  $R$

22

at present is calculated  $R = 13$  and rises to 18 at a CO<sub>2</sub> level of 800 ppm. This increase of  $R$



23 has been interpreted as indication of the collapse of the solubility pump. S and R, however,  
24 are defined from equilibrium chemistry and are a measure of the CO<sub>2</sub> absorbed by the  
25 ocean's upper mixed layer by increase of the CO<sub>2</sub> level in the atmosphere without regarding  
26 its sinking into the deep-ocean by the thermohaline circulation. The difference ΔDIC  
27 between the actual value and the value at 280 ppm is transported into the deep-ocean by  
28 the global meridional conveyor belt. ΔDIC increases with increasing CO<sub>2</sub> level. At 280 ppm  
29 the system ocean-atmosphere is in equilibrium and the sink is zero. At 400 ppm a value of  
30 about 1.9 Gtons/year is estimated that increases to 3.9 Gtons/year at 600 ppm and to 5  
31 Gtons/year at 800 ppm. At present CO<sub>2</sub> level increase of 2ppm/year 10 Gtons/year are  
32 absorbed by the ocean. The solubility pump contributes 3.2 Gtons/year: 1.3 Gtons/year by  
33 equilibrium absorption into the mixed layer and 1.9 Gtons/year by thermohaline circulation.  
34 At 600 ppm the total sink is 4.6 Gtons/year and at 800 ppm 5.5 Gtons/year. To conclude, the  
35 solubility pump is not endangered by ocean acidification. In contrast, it increases with  
36 increasing CO<sub>2</sub> level of the atmosphere to yield significant contribution.

37

### 38 **1. Introduction**

39 Only one half of anthropogenic CO<sub>2</sub> emitted remains in the atmosphere. About one quarter  
40 is absorbed by the land sink via vegetation. The remaining quarter sinks into the ocean by  
41 the biological pump and the physical (solubility pump) (Friedlingstein et al., 2022). The ocean  
42 CO<sub>2</sub> sink has increased steadily with rising CO<sub>2</sub> level since the beginning of industrialisation.  
43 As an example, CO<sub>2</sub> level of 317 ppm in 1960 raised to 420 ppm in 2021 and accordingly the  
44 ocean sink from 1.1 ± 0.4 GtC/yr in 1960 to 2.8 ± 0.4 GtC/ y during 2021 (Friedlingstein et al.,  
45 2022). Thus, the ocean sink has increased proportional to the rise in atmospheric CO<sub>2</sub>. To  
46 predict the future evolution of the CO<sub>2</sub>-concentration (ppm) in the atmosphere by models



47 one has to know whether this increase will be permanent. One part of the oceanic sink is the  
48 solubility pump that transports dissolved inorganic carbon (DIC) in equilibrium with the  
49 partial pressure  $p_{\text{CO}_2}$  in the atmosphere ( $0.0001 \text{ atm} \cong 100 \text{ ppm}$ ) into the deep ocean. The  
50 future effectivity of this physical pump has been questioned because with increasing  
51 acidification of the ocean its buffering capacity decreases. This is commonly expressed by  
52 the Revelle factor  $R$  (Zeebe and Wolf-Gladrow, 2001, Eglestone et al., 2010).

$$53 \quad R = (\Delta \text{DIC}/\text{DIC})/(\Delta \text{CO}_2/\text{CO}_2) = (\Delta \text{DIC}/\Delta \text{CO}_2)/(\text{DIC}/\text{CO}_2).$$

54  $\Delta \text{DIC}$  is the change in concentration DIC caused by a small increase  $\Delta \text{CO}_2$  of the  
55 concentration  $\text{CO}_2$  in the atmosphere.  $\text{CO}_2$  and DIC are the corresponding concentrations.

56 However, the Revelle factor is used mostly only qualitatively stating that increasing values  
57 of  $R$  indicate weakening of the buffer capacity (e.g., Climate Change 2007: The Physical  
58 Science Basis. AR4 IPCC, Bates and Johnson, 2020). A more appropriate measure, the  
59 sensitivity

60  $S = \Delta \text{DIC}/\Delta \text{CO}_2$  has not been used in the scientific community. Middelburg et al., 2020 state:

61 “there are few studies where buffer and/or sensitivity factors are being used, except for the  
62 well-known Revelle factor.” To judge quantitatively the decrease of buffer capacity that gives

63 the amount of DIC increase by reaction of  $\text{CO}_2$  to  $\text{HCO}_3^-$  and  $\text{CO}_3^{2-}$  the evolution of sensitivity  $S$   
64 in dependence on the  $\text{CO}_2$  level in the atmosphere is a better alternative. To this end I

65 calculate using the geochemical program PHREEQC (Parkhurst and Appelo, 2013) the

66 chemical composition of sea water in chemical equilibrium with  $\text{CO}_2$  of defined partial

67 pressure  $p_{\text{CO}_2}$  (ppm) in the surrounding atmosphere at defined temperature  $T$ . This way

68  $\text{DIC}(p_{\text{CO}_2}, T)$  as a function of  $p_{\text{CO}_2}$  and  $T$  is obtained. By differentiation one gets  $d\text{DIC}/dp_{\text{CO}_2}$

69  $= \Delta \text{DIC}/\Delta \text{CO}_2 = S$  at defined temperature. From this I discuss the decrease of buffer capacity

70 with increasing  $p_{\text{CO}_2}$ . I report the Revelle factor  $R$  as a function of  $S$  to enable quantitative



71 arguments using the Revelle factor R. This equilibrium pump does not consider the  
72 overturning circulation of the ocean that transports the water of the mixed zone into deep-  
73 ocean. This transport pump increases steadily with increasing  $p_{\text{CO}_2}$ . The physical pump is the  
74 sum of the sink by the equilibrium pump and the overturning transport pump. It increases  
75 steadily to yield significant contributions.

76

## 77 **Methods**

78 The input file of the program PHREEQC is shown in Table 1. The first block SOLUTION 1  
79 defines the composition of sea water including major elements and boron. The second block  
80 EQUILIBRIUM\_PHASES equilibrates this solution with gaseous  $\text{CO}_2$  of the surrounding  
81 atmosphere. Input parameters are temperature “temp” in °C and  $\text{CO}_2(\text{g})$  as  $\log(p_{\text{CO}_2})$  where  
82  $p_{\text{CO}_2}$  is in atm.

83 From the output file one can read pH and extract the concentrations of DIC (C(4)) and its

```
SOLUTION 1 Seawater
units ppm
pH 8.22
pe 8.451
density 1.023
temp 5
Ca 412.3
Mg 1291.8
Na 10768.0
K 399.1
Si 4.28
Cl 19353.0
B 4.5
Alkalinity 141.682
as HCO3
S(6) 2712.0
EQUILIBRIUM_PHASES
CO2(ag) -2.921
END
```

```
pH = 7.715
DIC C(4) 2.425e-03
HCO3- 1.753e-03
MgHCO3+ 3.129e-04
NaHCO3 2.253e-04
CO2 6.588e-05
CaHCO3+ 3.420e-05
8.017e-06
NaCO3 MgCO3
1.542e-05
CO3-2 -
5.031e-06
CaCO3 4.984e-06
```

84

85 **Table 1: Input file of PHREEQC**

**Table 2: Output results**

86 species in mol/kg. The program includes ion pairs with Ca and Mg.  $\text{MgHCO}_3^+$  and  $\text{NaHCO}_3$



87 occur in considerable concentrations. In programs that do not include ion pairs these are  
88 included as  $\text{HCO}_3^-$ . I have calculated DIC and pH from  $\text{CO}_2$  levels of 300 ppm in steps of  
89 33ppm up to 800 ppm. The data points were transferred to the program Origin. Then they  
90 were fitted to a 5<sup>th</sup> order polynomial ( $R$ -square = 0.99995;  $SD = 3,3 \cdot 10^{-4}$ ;  $p < 10^{-4}$ ) to smooth the  
91 data for differentiation performed by the program. The figures were created by the graphics  
92 of Origin.

93

### 94 3. Results

95 Fig.1 represents the results for DIC at fixed temperature  $T = 15^\circ\text{C}$  (solid line). The dashed line  
96 depicts the path where according to the increasing  $\text{CO}_2$  level the temperature increases

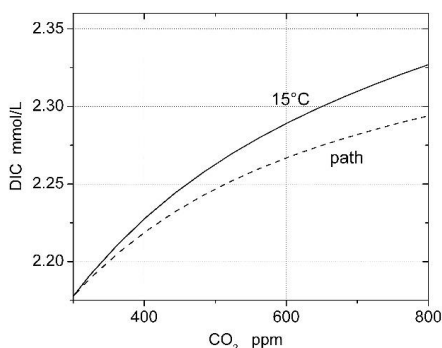


**Fig. 1: DIC at fixed temperature of  $T = 15^\circ\text{C}$  (solid line). The dashed line depicts DIC when temperature changes with increasing  $\text{CO}_2$**

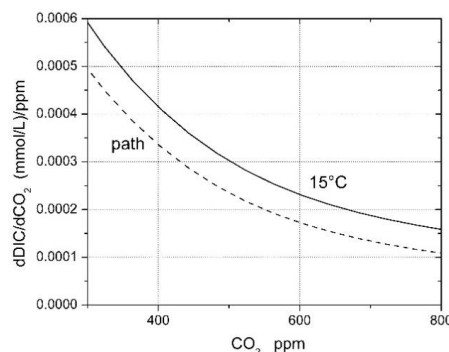


**Fig. 2: Sensitivity  $S = d\text{DIC}/d\text{CO}_2$  for fixed temperature (solid line) and the path (dashed line) taking into account temperature increase with increasing  $\text{CO}_2$  level. See text.**

97 linearly by  $0.01^\circ\text{C}$  per 1ppm increase of  $\text{CO}_2$  level corresponding to their linear correlation  
98 obtained from NASA data of temperature and  $\text{CO}_2$  level. The curve starts at  $T = 15^\circ\text{C}$ , 300  
99 ppm with steps of 33 ppm and  $0.34^\circ\text{C}$  and ends at 800 ppm and  $T = 19.1^\circ\text{C}$ . Due to the rising  
100 temperature DIC is reduced slightly in comparison to fixed temperature at  $15^\circ\text{C}$ . Fig 2  
101 depicts the sensitivity  $S = d\text{DIC}/d\text{CO}_2$  obtained from differentiation of the curves in Fig. 1.



102 dDIC is the change in the concentration of DIC in mmol/L that is caused by an increase of CO<sub>2</sub>  
 103 by dCO<sub>2</sub> in ppm. This change can be converted as change of the aqueous CO<sub>2</sub> concentration  
 104 c<sub>aq</sub> in the liquid by Henry's law  $c_{aq} = K_H \cdot p_{CO_2}$ . At 15°C for sea water,  $K_H = 0.04$  mol/atm  
 105 (Zeebe and Wolf-Gladrow,2001). For 1ppm the change  $dc_{aq} = 4 \cdot 10^{-5}$  mmol CO<sub>2</sub><sup>aq</sup>. The  
 106 corresponding change  $dDIC = S \cdot 1ppm = 0.0004$  mmol DIC. Defining S\*in units of  
 107 mmolDIC/mmolCO<sub>2</sub><sup>aq</sup> this way  $S^* = 0.0004/0.00004$  mmolDIC/mmol CO<sub>2</sub><sup>aq</sup> = 10

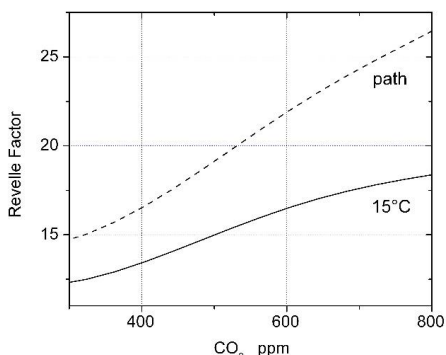


**Fig. 3: Revelle factor for fixed temperature (solid line) and path (dashed line).**

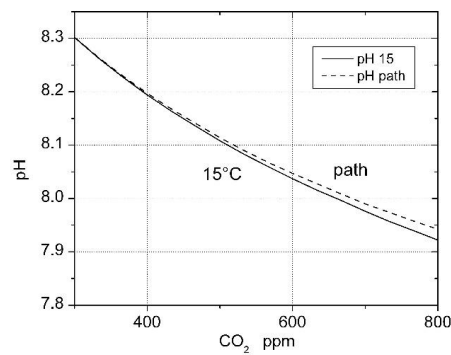


**Fig. 4: pH for fixed temperature (solid line) and path (dashed line).**

108  
 109 mmolDIC/mmolCO<sub>2</sub><sup>aq</sup> at 400 ppm. This means that 10 units CO<sub>2</sub> have been absorbed of  
 110 which 9 units have reacted to carbonates. For low pH < 4 where all DIC is in CO<sub>2</sub><sup>aq</sup>, S\* = 1. At  
 111 15°C the value of S = 0.0001 corresponds to value S\* = 2.5. Note that this conversion  
 112 depends on temperature due to the temperature dependence of K<sub>H</sub> (0.051 at 5°C, 0.038 at  
 113 15°C. and 0.029 at 5°C). Both sensitivity curves show a steady drastic decline of the buffering  
 114 capacity from 0.0006 to 0.00016 (mmol/L)/ppm at fixed temperature and from 0.0005 to  
 115 0.00011 (mmol/L)/ppm for the path. Thus, the reduction by doubling CO<sub>2</sub> from 300 ppm to  
 116 600 ppm means a reduction to 42 % at fixed temperature and 33 % for the path.  
 117 The corresponding Revelle factors  $R = (DIC/CO_2)/(dDIC/dCO_2)$  are shown in Fig. 3. They



118 illustrate why the Revelle factor cannot be used easily as quantitative measure because the  
119 reduction of buffer capacity is by its change and not by its absolute value. Therefore, one has  
120 to know the end values. In contrast, sensitivity  $S$  gives the reduction from the known initial  
121 value. In other words, the large background of  $R$  at 300 ppm prevents a reasonable  
122 interpretation. Finally, in Fig. 4 acidification of ocean, the reason for declining buffer capacity  
123 is shown as pH versus  $\text{CO}_2$  level. pH drops almost linearly with  $\text{CO}_2$  level from pH = 8.3 at 300  
124 ppm to 7.9 at 800 ppm. There is little difference between constant temperature at 15°C and  
125 the path regarding global warming. The change in pH is close to the projection of Jiang et al.,  
126 2019 using the RCP 6.0 scenario of IPCC. This holds also for the change of the Revelle factor  
127  $R$  in Fig. 3.

128

#### 129 4. Discussion

130 To obtain some overview on the variability of sensitivity  $S$  and Revelle factors  $R$  in Fig. 5 one  
131 finds DIC for 5, 15, and 25°C respectively. The corresponding sensitivities  $S$  are shown in Fig.  
132 6 and the Revelle factors are depicted in Fig. 7. For completion pH is illustrated in Fig. 8.

133

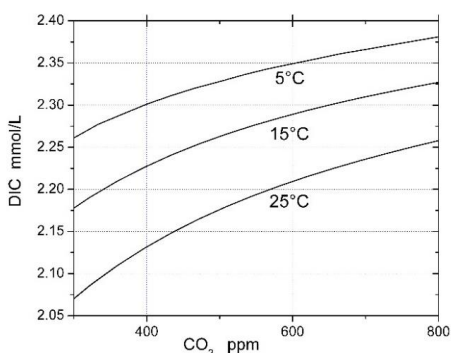


**Fig. 5: DIC concentration for various temperatures**

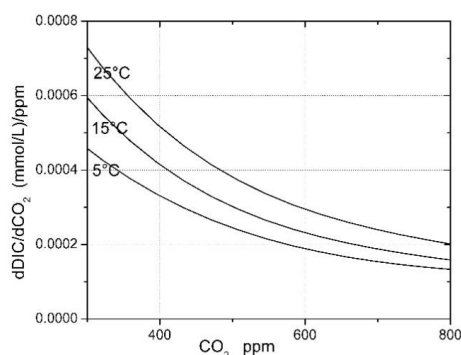


**Fig. 6: Sensitivity  $S = d\text{DIC}/d\text{CO}_2$  for various temperatures**



134 At fixed CO<sub>2</sub> the DIC concentration (Fig. 5) decreases with temperature whereas the  
135 sensitivity  $S$  increases as can be seen from the slopes increasing with rising temperature.  
136 These slopes are shown as  $S = dDIC/dCO_2$  in Fig. 6.  $S$  increases with rising temperature. As  
137 one can read from Fig. 6 an increase of temperature by 5°C causes a reduction of the initial  
138 value at 15°C by about 10% for all CO<sub>2</sub> levels. The impact of changing CO<sub>2</sub> level by far exceeds  
139 that of increasing temperature.  
140  $S$  decreases with increasing CO<sub>2</sub> level. It is important to note that one finds a reduction by 36  
141 % at the beginning from 300 to 420 ppm, corresponding to the time from 1945 to 2021.  
142 Further reduction from 400 to 500 ppm is 16 % and continues to decrease further on for all  
143 temperatures. This is in contrast to the opposite behaviour of the Revelle factor in Fig. 7.  
144 One finds a small increase at the beginning up to 400 ppm followed by rise about twice of  
145 the initial one for CO<sub>2</sub> between 400 to 600 ppm, valid for all temperatures. Thus, using  $S$  as  
146 measure for impact to the oceans buffer capacity leads to conflictive conclusion about future

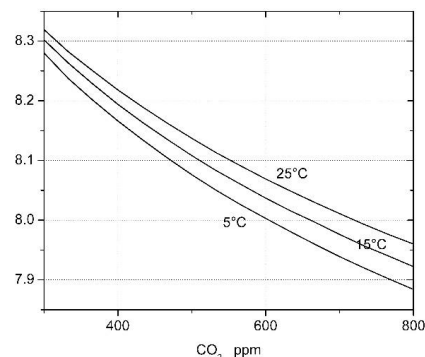
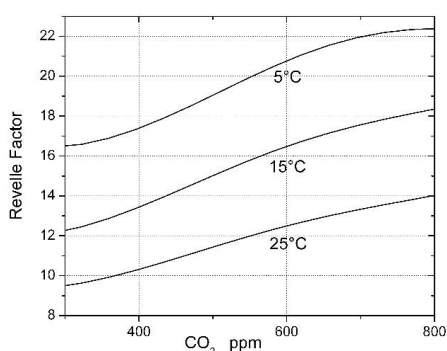


**Fig. 7: Revelle factor for various temperatures**    **Fig. 8: pH for various temperatures.**

147 evolution with consequences in defining pathways for CO<sub>2</sub> emissions in climate change  
148 policy. At present public policy seems to be convinced that at least the physical ocean pump  
149 will fail in the near future. Although the mixed layers capacity has been reduced by about  
150 30% of its initial value for all temperatures during 1945 (300ppm) to 2015 (400ppm). The





151 ocean sink (Friedlingstein et al., 2022), however has continuously increased during this time  
 152 span. This leads to the conjecture that the physical sink into the mixed layer may not  
 153 contribute as significantly to the total ocean sink as thought by using the concept of  
 154 equilibrium chemistry (Revelle factor).  
 155 Finally, to relate sensitivity  $S$  to Revelle factor  $R$ , Fig. 9 illustrates  $R$  as a function of  $S$ .

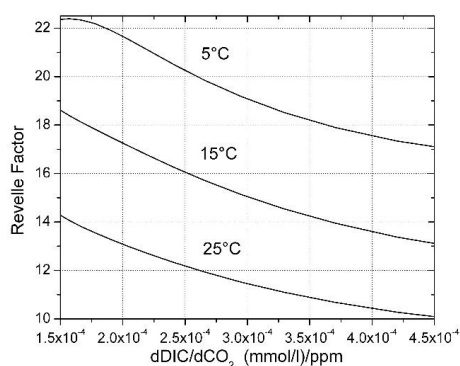


**Fig. 9: The Revelle factors  $R$  in relation to the sensitivity  $S$  for various temperatures**

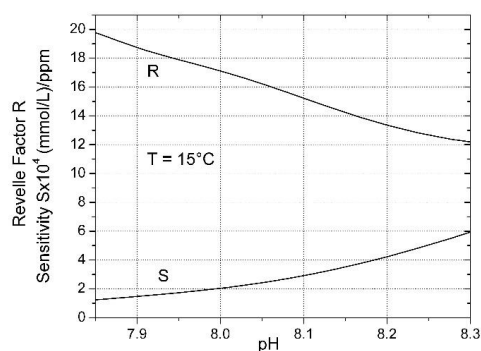


**Fig. 10: The Revelle factor  $R$  and sensitivity  $S$  as function of  $pH$  at 15°C**

156 It is obvious why using  $S$  should be preferred. If  $S$  changes from  $1.5 \cdot 10^{-4}$  to  $4.5 \cdot 10^{-4}$  by 200 %  
 157 the corresponding change in  $R$  is only about 40 % for 25°C and 20% for 5°C. Therefore,  $S$  gives  
 158 a more realistic view. Fig. 10 shows  $R$  and  $S$  as function of  $pH$  at 15°C.  $R$  changes from 12 to  
 159 20 with  $pH$  decreasing from 8.3 to 7.85. But, in contrast to the sensitivity from its value no  
 160 direct meaning can be derived. From its definition a simple relation is:  $R = 2.27 / (CO_2 \cdot S)$   
 161 because  $DIC \approx 2.27$  mmol/L remains constant within a few percent (see Fig. 1 and Fig. 5).  
 162 From this one may understand why  $R$  is used only qualitatively to judge ocean's physical  
 163 pump buffer capacity.  
 164 Using the DIC data one can estimate the upper limit of the present  $CO_2$  flux from the  
 165 atmosphere to the ocean's mixed layer. I calculate the volume  $V_1$  of the upper 1 meter of the  
 166 mixed layer  $V_1 = 0.71 \cdot 4\pi R^2 \cdot 1 \text{ m}^3 = 3.6 \cdot 10^{17} \text{ L}$ .  $R$  is Earth radius and 0.71 ocean coverage. The



167 amount  $M_1$  of DIC that can be absorbed with a sensitivity  $S_1 = 10^{-7}(\text{mol/L})/\text{ppm}$  is  $M_1 = V_1 \cdot S_1$   
168 mol/ppm. Consequently, the amount  $M_t$  absorbed by a mixed layer with depth  $t(\text{m})$  and a  
169 change of  $n$  ppm  $\text{CO}_2$  is  $M_t = M_1 \cdot t \cdot s \cdot n$  mol  $\text{CO}_2$  when sensitivity  $S = s \cdot S_1$ . Converting to g  $\text{CO}_2$   
170 one has to multiply by the molecular weight 44 g/mol of  $\text{CO}_2$  to obtain  
171  $M_t = M_1 \cdot t \cdot s \cdot n$  mol  $\cdot 44\text{g/mol} = M_1 \cdot t \cdot s \cdot n \cdot 44$  (g).  
172 A reasonable estimation of the mixed layer depth  $t$  is 100 m (de Boyer et al., 2004, Boyer et  
173 al., 2022, Birol Kara et al., 2000, Doney et al., 2004). At present the increase of  $\text{CO}_2$  is  
174 2 ppm/year ( $n = 2$ ) and ( $s = 4$ ). Using these numbers, one finds  $M_t = 1.3$  Gigatons/year. The  
175 value of  $s = 4$  corresponds to a temperature of  $15^\circ\text{C}$  at 420 ppm (see Fig. 6). This assumption  
176 is reasonable because oceans temperature is distributed between  $25^\circ$  at the equator to  $5^\circ\text{C}$   
177 in the polar oceans.  
178 Another argument must also be considered. Carbon is absorbed by the ocean where water  
179 sinks to the deep ocean. At regions of upwelling water rich in  $\text{CO}_2$ , however,  $\text{CO}_2$  is released  
180 into the atmosphere (Landschützer et al., 2014, Crisp et al., 2022). This water outgasses  $\text{CO}_2$   
181 into an atmosphere with higher partial pressure. This causes a reduced flux of outgassing  
182 and the difference of outgassing between higher and lower partial pressure at the intake  
183 acts as effective influx in upwelling regions and justifies the assumption.  
184 It must be stressed that the flux calculated so far by equilibrium chemistry represents the  
185 capacity to absorb  $\text{CO}_2$  from the atmosphere by a stagnant isolated mixed layer that does  
186 not sink into depth. Therefore, this sink is caused by equilibrium chemistry and could be  
187 termed as equilibrium sink (pump). This pump declines with increasing acidification of the  
188 ocean. At  $\text{pH} < 4$  the only existing carbonate species are aqueous  $\text{CO}_2$  and  $\text{H}_2\text{CO}_3$ . Therefore,  
189 the absorption of  $\text{CO}_2$  is governed by Henry's law. Therefore,  $d\text{DIC}/d\text{CO}_2 = K_H$  and stays  
190 constant with further decreasing pH. At  $15^\circ\text{C}$   $d\text{DIC}/d\text{CO}_2 = 4 \cdot 10^{-5}$  mmol/ppm. This



191 corresponds to a flux of 0.13 Gt/year, an almost total breakdown of the mixed layer's  
192 capacity to absorb CO<sub>2</sub>.

193 This, however, does not mean that the physical pump breaks down as has been concluded  
194 from the increase of the Revelle factor. In IPCC AR4 one finds: "The ocean's capacity to  
195 buffer increasing atmospheric CO<sub>2</sub> will decline in the future as ocean surface pCO<sub>2</sub> increases  
196 (Figure 7.11a). This anticipated change is certain, with potentially severe consequences."  
197 (Denman et al., 2007).

198 The total CO<sub>2</sub> sink consists of two parts: the equilibrium sink as already stated and the  
199 transport sink. This is governed by the global meridional overturning circulation where  
200 surface waters of the mixed layer flow from the equator to the polar regions and sink there  
201 into the deep ocean by thermohaline circulation. In the North Atlantic deep water formation  
202 is 15±2 Sv (1 Sv = 10<sup>6</sup> m<sup>3</sup>/s) and 21±6 Sv in the southern ocean (Ganachaud and Wunsch,  
203 2000, Rahmstorf, 2002). These waters have cooled to low temperatures (about 5°C) when  
204 they sink. They transfer the CO<sub>2</sub> in the mixed layer that contains also the anthropogenic  
205 carbon into deep-ocean. These waters are replaced by upwelling waters back to the surface  
206 without anthropogenic carbon (Terhaar et al., 2022) that readily absorb CO<sub>2</sub> from the  
207 atmosphere until equilibrium is established.

208 Dividing the volume  $V_{\text{mix}}$  of the mixed layer by the global formation of deep water of 36±6 Sv  
209 one obtains,  $\tau_{\text{drain}}$ , the time needed to drain that layer into the ocean as 57 years. The time  
210 for chemical equilibration to a change of atmospheric CO<sub>2</sub> is on the order of 1 year (Jones et  
211 al., 2014). Therefore, DIC in the mixed layer is in equilibrium with the CO<sub>2</sub> in the atmosphere  
212 as given in Fig.5. At a CO<sub>2</sub> level of 280 ppm the flux of CO<sub>2</sub> into the ocean is zero and the  
213 system is in equilibrium (Friedlingstein et al., 2022). With increasing CO<sub>2</sub> level, the deviation  
214 of DIC equilibrium concentration is given by  $(\text{DIC}_{\text{ppm}} - \text{DIC}_{280}) = \Delta\text{DIC}_{\text{ocean}}$ .  $\Delta\text{DIC}_{\text{ocean}}$  represents



215 the amount of anthropogenic carbon absorbed into the mixed layer since the onset of  
 216 industrialisation. The flux  $F_{\text{ocean}}$  into the ocean is given by  $\Delta\text{DIC} \cdot V_{\text{mix}} / \tau_{\text{drain}} = F_{\text{ocean}}$  in  
 217 Gtons/year. At 400 ppm one finds a value of  $F_{\text{ocean}} = 1.9$  Gtons/year

218 Fig. 9 depicts  $F_{\text{ocean}}$  in dependence on the  $\text{CO}_2$  level.  $F_{\text{ocean}}$  does not increase linearly with  $\text{CO}_2$

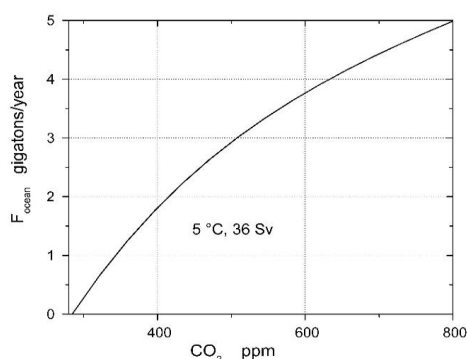


**Fig. 11: Flux  $F_{\text{ocean}}$  into the ocean in dependence on  $\text{CO}_2$  level**

level but increases with declining slope to 0.0087 Gtons/(year ppm) that stays constant for  $p_{\text{CO}_2} > 1$  atm as calculated by PHREEQC. This way for an increase of 1 ppm/year of  $\text{CO}_2$  level,  $F_{\text{ocean}}$  increases by 0.0087 Gtons/year.

227 At present the total Ocean sink is 10 Gt/year. If at 400 ppm a total sink of 3.2 Gt/year is  
 228 correct the contribution of the physical pump is relatively small. It is possible that the  
 229 biological pump (Hauck and Völker, 2015, Riebesell et. al., 2007) compensates for this. In  
 230 view of the fact that this estimation might be critiqued it should motivate further research  
 231 and discussion in ongoing projects.

232

### 233 5. Conclusion

234 An alternative measure of the ocean's carbonate buffer to absorb  $\text{CO}_2$  from the atmosphere  
 235 is proposed. Instead of the Revelle factor  $R = (\Delta\text{CO}_2/\text{CO}_2) / (\Delta\text{DIC}/\text{DIC}) = (\text{DIC}/\text{CO}_2) /$   
 236  $(\Delta\text{DIC}/\Delta\text{CO}_2)$  the sensitivity  $S = (\Delta\text{DIC}/\Delta\text{CO}_2)$  is preferable because it gives directly the  
 237 change  $\Delta\text{DIC}$  of the concentration of DIC in the seawater caused by the change  $\Delta\text{CO}_2$  of  
 238 carbon dioxide level in the atmosphere. To this end the DIC concentration of seawater in



239 equilibrium with a defined CO<sub>2</sub> level in the surrounding atmosphere is calculated by use of  
240 the geochemical program PHREEQC. From the function DIC(CO<sub>2</sub>) by derivation one obtains  
241 the sensitivity  $S = dDIC/dCO_2 = \Delta DIC/\Delta CO_2$  and also the Revelle factor R.  
242 Using S, the change of the ocean's buffer capacity better insight of its future evolution is  
243 obtained than by use of the Revelle factor R.  
244 S declines heavily since 1945 until it breaks down at CO<sub>2</sub> levels of 800ppm. One has to  
245 consider, however, that R and S are calculated by equilibrium chemistry that does not  
246 contain the sink caused by the thermohaline overturning circulation that transports the  
247 water of the mixed zone into deep-ocean. S therefore, gives the amount of carbon as  $\Delta DIC$   
248 that is stored in the mixed layer when the CO<sub>2</sub> level increases by  $\Delta CO_2$ .  
249 The total solubility sink consists of two mechanisms: The equilibrium pump as described and  
250 the transport pump that is caused by the global meridional overturning circulation of 36 Sv.  
251 This transfers into deep-ocean the difference  $(DIC_{ppm} - DIC_{280}) = \Delta DIC_{ocean}$  that has been  
252 accumulated in the mixed layer from onset of industrialisation to the actual CO<sub>2</sub> level.  
253 This sink increases continuously replacing the failure of the equilibrium pump. At 400 ppm  
254 the total sink is 1.9, at 600 ppm it is 3.8 and at 800 ppm it amounts to 5 Gtons/year  
255 depending solely on the CO<sub>2</sub> level in the atmosphere for ppm > 600.  
256 To conclude, the total solubility pump is not endangered by ocean acidification. In contrast,  
257 it increases with increasing CO<sub>2</sub> level of the atmosphere to yield significant contribution to  
258 remove anthropogenic CO<sub>2</sub> from the atmosphere into deep-ocean.

259

260 **I declare that I do not have any competing interests.**

261

262 **References**



- 263 Bates, N.R., Johnson, R.J. Acceleration of ocean warming, salinification, deoxygenation and  
264 acidification in the surface subtropical North Atlantic Ocean. *Commun Earth Environ* 1, 33  
265 2020. <https://doi.org/10.1038/s43247-020-00030-5>  
266 Crisp D., Dolman H., Tanhua T., McKinley G. A., Hauck J., Bastos A., Sitch S., Eggleston S., Aich  
267 V. How Well Do We Understand the Land-Ocean-Atmosphere Carbon Cycle?, *Reviews of*  
268 *Geophysics* / Volume 60, Issue 2 / e2021RG000736, 2022  
269 <https://doi.org/10.1029/2021RG000736>  
270 de Boyer Montégut Clément, Gurban M., Fischer A. S., Lazar A., Iudicone D. Mixed layer  
271 depth over the global ocean: An examination of profile data and a profile-based climatology.  
272 *Journal Of Geophysical Research-oceans*, 109(C12/C12003), 1-20.2004  
273 <https://doi.org/10.1029/2004JC002378>  
274 de Boyer Montégut Clément (2022). Mixed layer depth climatology computed with a density  
275 threshold criterion of 0.03kg/m<sup>3</sup> from 10 m depth value. SEANOE.  
276 <https://doi.org/10.17882/91774>  
277 Denman, K.L., G. Brasseur, A. Chidthaisong, P. Ciais, P.M. Cox, R.E. Dickinson, D.  
278 Hauglustaine, C. Heinze, E. Holland, D. Jacob, U. Lohmann, S Ramachandran, P.L. da Silva  
279 Dias, S.C. Wofsy and X. Zhang, 2007: Couplings Between Changes in the Climate System and  
280 Biogeochemistry. In: *Climate Change 2007: The Physical Science Basis. Contribution of*  
281 *Working Group I to the Fourth*  
282 *Assessment Report of the Intergovernmental Panel on Climate Change* [Solomon, S., D. Qin,  
283 M. Manning, Z. Chen, M. Marquis, K.B. Averyt, M.Tignor and H.L. Miller (eds.)]. Cambridge  
284 University Press, Cambridge, United Kingdom and New York, NY, USA .2007  
285 Doney S. C. et al., Evaluating global ocean carbon models: The importance of realistic  
286 physics, *GLOBAL BIOGEOCHEMICAL CYCLES*, VOL. 18, GB3017, 2004  
287 Eggleston E. S., Sabine C., Francois M. M., Morel F. M. M., Revelle revisited: Buffer factors that  
288 quantify the response of ocean chemistry to changes in DIC and alkalinity.  
289 *Global Biogeochemical Cycles*, *Global Biogeochemical Cycles*, Volume 24, Issue 1, 2010  
290 <https://doi.org/10.1029/2008GB003407>  
291 Friedlingstein P. 2015 Carbon cycle feedbacks and future climate change. *Phil. Trans. R. Soc.*  
292 *A* 373: 20140421. 2015  
293 Ganachaud, A. & Wunsch, C. Improved estimates of global ocean circulation, heat transport  
294 and mixing from hydrographic data. *Nature* 408, 453–457 (2000).  
295 Hauck J., Völker C. Rising atmospheric CO<sub>2</sub> leads to large impact of biology on Southern  
296 Ocean CO<sub>2</sub> uptake via changes of the Revelle factor *Geophysical Research Letters* *Volume 42*,  
297 *Issue 5* p. 1459-1464, 2015 <https://doi.org/10.1002/2015GL063070>  
298 Jiang L-Q., Carter B.R., Feely R. A., Lauvse S. K., Olsen A. Surface Ocean pH and buffer  
299 capacity: past, present and future. *Scientific Reports*, 9:18624, 2019  
300 <https://doi.org/10.1038/s41598-019-55039-4>  
301 Jones, D. C., T. Ito, Y. Takano, and W.-C. Hsu (2014), Spatial and seasonal variability of the  
302 air-sea equilibration timescale of carbon dioxide, *Global Biogeochem. Cycles*, 28, 1163–1178,  
303 doi:10.1002/2014GB004813  
304 Kara A. B., Peter A. Rochford, Harley E. Hurlburt. An optimal definition for ocean mixed layer



305 Landschützer P., Gruber N., Bakker D. C. E., Schuster. Recent variability of the global ocean  
306 carbon sink. *Global Biogeochemical Cycles*, 28, 927-949, 2014

307 Köhler P., Hauck J., Völker C., Wolf-Gladrow D. Interactive comment on “A simple model of  
308 the anthropogenically forced CO<sub>2</sub> cycle” by W. Weber et al., *Earth Syst. Dynam. Discuss.*, 6,  
309 C813–C813, 2015. [www.earth-syst-dynam-discuss.net/6/C813/2015/](http://www.earth-syst-dynam-discuss.net/6/C813/2015/)

310 Middelburg J. J., Soetaert K., Hagens M. Ocean Alkalinity, Buffering and Biogeochemical  
311 Processes, *Reviews of Geophysics*, Volume 58, Issue 3 / 2020  
312 <https://doi.org/10.1029/2019RG000681>

313 Parkhurst, D.L., and Appelo, C.A.J., 2013, Description of input and examples for PHREEQC  
314 version 3—A computer program for speciation, batch-reaction, one-dimensional transport,  
315 and inverse geochemical calculations: U.S. Geological Survey Techniques and Methods, book  
316 6, chap. A43, 497 p., available only at <http://pubs.usgs.gov/tm/06/a43>.

317 Rahmstorf S. Ocean circulation and climate during the past 120,000 years. 2002, *NATURE*  
318 419, 207-214

319 Zhang X., 2007: Couplings Between Changes in the Climate System and Biogeochemistry. In:  
320 *Climate Change 2007: The Physical Science Basis. Contribution of Working Group I to the*  
321 *Fourth Assessment Report of the Intergovernmental Panel on Climate Change* [Solomon, S.,  
322 D. Qin, M. Manning, Z. Chen, M. Marquis, K.B. Averyt, M. Tignor and H.L. Miller (eds.)].  
323 Cambridge University Press, Cambridge, United Kingdom and New York, NY, USA. 2007

324 Terhaar J., Frölicher T. L., Joos F. Observation-constrained estimates of the global ocean  
325 carbon sink from Earth system models. *Biogeosciences*, 19, 4431–4457, 2022  
326 <https://doi.org/10.5194/bg-19-4431-2022>

327 Zeebe R. E. and Wolf-Gladrow D. CO<sub>2</sub> IN SEAWATER: EQUILIBRIUM, KINETICS, ISOTOPES,  
328 Elsevier Oceanography Series, 65, 2001

329